Electronic specific heat in metallic Van Vleck paramagnets

Koji Akai
Department of Physics, Faculty of Science, Osaka City University, Sumiyoshiku, Osaka 558, Japan

Hiroumi Ishii
Department of Material Science, Faculty of Science, Osaka City University, Sumiyoshiku, Osaka 558, Japan
(Received 7 December 1992; revised manuscript received 3 August 1993)

Electronic specific heat due to virtual excitation of the crystal-field singlet ground state is studied by including higher-order processes, following the Doniach-Engelsberg-Brinkman theory. As the effective electron-electron interaction mediated by the excitation of the crystal-field states turns repulsive near the Fermi surface, correspondence with the Hubbard model is investigated. The specific heat is separated into a fermionlike term and a bosonlike term. The former has a T-linear contribution which corresponds to that in the Hubbard model. The bosonlike term corrects the Schottky-type contribution of individual crystal-field states by their collective modes. Numerical calculation is made in a simplified model for real substances to see the relative size of the fermion and boson terms in a magnetic field.

I. INTRODUCTION

In the rare-earth metals of non-Kramers ions such as Pr and their intermetallic compounds, a singlet ground state for the localized f electrons is brought about by the crystal field. Many of these substances have energy splittings on the order of several tens of K and remain paramagnetic even in the presence of exchange interaction.[1]

Although the singlet ground state is thermally inactive at low temperatures, its virtual excitation described by the Van Vleck susceptibility yields effective interactions among nuclear spins and conduction electrons through the hyperfine interaction and the s-f exchange interaction. For example, a process in which a nuclear spin excites the singlet ground state and the Zeeman field returns it back yields the enhanced Zeeman energy for the nuclear spin. Similarly, hyperfine-enhanced interaction between nuclear spins arises through a process in which the excitation of the singlet ground state due to a nuclear spin is transferred to neighboring sites by an electron-hole pair excitation of conduction electrons. The enhanced nuclear magnetism is one of the main problems in ultralow-temperature physics.[2]

On the other hand, a process in which a conduction electron excites the crystal-field state and puts it back to the ground state yields the self-energy of the conduction electron. White and Fulde,[3] and Fulde and Jensen[4] calculated the excess specific heat due to this self-energy and gave the explanation for the strong magnetic field dependence of the specific heat found in Pr metal by Forgan.[5] The mass enhancement in the Pr metal is also found in the cyclotron mass by means of the de Haas–van Alphen effect by Wulff *et al.*[6] To analyze the result these authors estimated the mass enhancement by using the random-phase-approximation (RPA) susceptibility to include the higher-order processes.

When an electron excites the crystal-field state and another electron puts it back, the process turns to the indirect interaction between these two electrons. This indirect electron-electron interaction and effects resulting from it have been studied by us.[7–9] It has been shown there that the indirect interaction $I_{\rm eff}$ is proportional to the ω-dependent Van Vleck susceptibility multiplied by the square of s-f exchange integral. It is short range repulsion for electrons near the Fermi surface, but turns attractive for the energy larger than crystal-field splitting. The similarity of the interaction for the electrons near the Fermi surface to that in the Hubbard model turns to a clue for the study of susceptibility, nuclear relaxation rate, specific heat, etc. The RPA susceptibility has been also used to include the higher-order processes of excitation of the crystal field state.

The specific heat in the Hubbard model has been studied by Doniach and Engelsberg,[10] Brinkman and Engelsberg,[11] and Brenig, Mikeska, and Riedel.[12] They derived the mass enhancement, which shows logarithmic singularity at the ferromagnetic instability and the $T^3 \ln T$ term as the next leading term. It is interesting to see in what extent correspondence holds in specific heat between the metallic Van Vleck paramagnets and the Hubbard model as a result of their similarity. To clarify this point is the first purpose of the present paper. We follow the Doniach-Engelsberg-Brinkman theory. The specific heat is separated into a fermionic term and a bosonic term. It will be shown that the T-linear term agrees with the result of the Hubbard model by replacing the repulsion I with $I_{\rm eff}$. The next dominant term is proportional to T^3. The $T^3 \ln T$ term corresponding to the Doniach-Engelsberg theory is much smaller than the T^3 term by the factor of crystal-field splitting divided by the Fermi energy. With increasing temperature the ω dependence of $I_{\rm eff}$ turns more important and the correspondence with the Hubbard model is lost. In Ref. 9, we have reported parts of this result without giving the derivation.

The second purpose of this paper is to show directly

from the s-f exchange model that the contribution of the bosonic term leads to the specific heat of the collective excitation modes of the crystal-field states. Energy levels of the isolated crystal levels turn to the band, and the energy gap reduces. The onset temperature of the Schottky specific heat deduces to cover the fermionic contribution. To see the relative size of the fermion contribution with respect to the bosonic one, we make numerical calculation for a simplified model for real substances in a magnetic field. The strong field dependence is characteristic of the present system.

In Sec. II, after describing the effective Hamiltonian obtained in the previous papers,[7,9] we apply the formalism of Brinkman and Engelsberg[11] on the electronic specific heat to the present problem. In Sec. III, on the basis of this, we calculate the specific heat of the fermionic term in a series expansion of T. A comparison with the result of Doniach and Engelsberg is made. Next we study the contribution of the bosonic term. In the last section a summary and discussion are made briefly.

II. HAMILTONIAN

We start our study by writing the Hamiltonian of the system consisting of the conduction electrons and the non-Kramers ions in the crystal field,

$$H=\sum_{\mathbf{k}\sigma}\varepsilon_{\mathbf{k}}c^{\dagger}_{\mathbf{k}\sigma}c_{\mathbf{k}\sigma}+\sum_{i,n}E_n|i,n\rangle\langle i,n|-g_J\mu_B\mathbf{H}\cdot\sum_i\mathbf{J}_i$$
$$-\frac{\tilde{J}_{s\text{-}f}}{2N}\sum_{\mathbf{k}\mathbf{k}'}\sum_i e^{i(\mathbf{k}-\mathbf{k}')\cdot\mathbf{R}_i}\sum_{\alpha,\alpha'}c^{\dagger}_{\mathbf{k}'\sigma'}\boldsymbol{\sigma}_{\alpha'\alpha}\cdot\mathbf{J}_i c_{\mathbf{k}\sigma}\ , \tag{2.1}$$

where $c_{k\sigma}$ is the annihilation operator of the conduction electron with wave vector $\mathbf{k}$ and spin σ, ε_k is its one-electron energy, $|i,n\rangle$ represents the nth crystalline field state at the site i with the energy E_n. Especially we represent the singlet ground state and its energy by $|i,g\rangle$ and E_g. The last two terms of (2.1) are the Zeeman energy of the non-Kramers ions and the s-f exchange interaction. $\tilde{J}_{s\text{-}f}$ denotes the s-f exchange coupling constant $J_{s\text{-}f}$ multiplied by (g_J-1). Note that $J_{s\text{-}f}$ is equal to $2I$, where I is defined as the s-f exchange constant in Refs. 3, 4, and 6. N is the total number of the non-Kramers ions, σ are the Pauli matrices for the conduction electron and $\mathbf{J}_i$ is the total angular momentum of non-Kramers ion at the ith site.

As the excitation energy of the crystal field state, $E_n-E_g\equiv E_{ng}$, is usually of the order of several tens of K, the non-Kramers ions are in the singlet ground state in low temperatures. The effect on the conduction electrons appears through their virtual excitation by the s-f exchange interaction. The effective interaction for the conduction electrons is obtained[7,9] by the canonical transformation as

$$V_{\text{eff}}=\frac{1}{2N}\sum_{\mathbf{k}_1\mathbf{k}_2\mathbf{q}}\sum_{\alpha_1\sim\alpha_4}I_{\alpha_1\alpha_2\alpha_3\alpha_4}(\varepsilon_{\mathbf{k}_1+\mathbf{q}}-\varepsilon_{\mathbf{k}_1})c^{\dagger}_{\mathbf{k}_1+\mathbf{q}\alpha_1}c_{\mathbf{k}_1\alpha_2}c^{\dagger}_{\mathbf{k}_2-\mathbf{q}\alpha_3}c_{\mathbf{k}_2\alpha_4}\ , \tag{2.2}$$

$$I_{\alpha_1\alpha_2\alpha_3\alpha_4}(\omega)=-\frac{\tilde{J}^2_{s\text{-}f}}{4}\sum_{\mu\nu=xyz}\langle\alpha_1|\sigma_\mu|\alpha_2\rangle\chi^{(0)\mu\nu}_f(\omega)\langle\alpha_3|\sigma_\nu|\alpha_4\rangle\ , \tag{2.3}$$

where $\chi^{(0)\mu\nu}_f$ is the Van Vleck susceptibility in a unit of $(g_J\mu_B)^2$ at $T=0$ given by

$$\chi^{(0)\mu\nu}_f(\omega)=\sum_n\left[\frac{\langle g|J^\mu|n\rangle\langle n|J^\nu|g\rangle}{E_{ng}-\hbar\omega}+\frac{\langle g|J^\nu|n\rangle\langle n|J^\mu|g\rangle}{E_{ng}+\hbar\omega}\right]. \tag{2.4}$$

If $I_{\alpha1\sim\alpha4}(\omega)$ is replaced by $I_{\alpha1\sim\alpha4}(0)$, V_{eff} turns to the short range repulsive interaction,

$$V^{(0)}_{\text{eff}}=I\sum_j n_{j\uparrow}n_{j\downarrow}+\frac{I}{2}\sum_j(n_{j\uparrow}+n_{j\downarrow})\ , \tag{2.5}$$

with

$$I=\frac{\tilde{J}^2_{s\text{-}f}}{4}\sum_{\mu=xyz}\chi^{(0)\mu\mu}_f(0)\ . \tag{2.6}$$

Then the result obtained in the Hubbard model[10-12] can be used at once. However, the ω dependence of $I_{\alpha1\sim\alpha4}(\omega)$ is due to that of the Van Vleck susceptibility and reflects the crystal-field splitting. Therefore, although one may use $I(0)$ at energy or temperature much lower than the crystal-field splitting to discuss the mass-enhancement or T-linear specific heat, it is necessary to consider this ω dependence for further study beyond this region. It is rather interesting to clarify how the specific heat of the present system differs from that of the Hubbard model with increasing temperature. Accordingly we extend our study following the formalism for the Hubbard model by Engelsberg and Brinkman.[11]

III. SPECIFIC HEAT BY RPA

Our purpose in this section is to give an expression of the electronic specific heat for the Hamiltonian (2.1).

The excess thermodynamic potential $\Delta\Omega$ due to the s-f exchange interaction is given by the following standard formula expressed by the coupling-constant integration,

$$\Delta\Omega=\lim_{\tau\to-0}\frac{2}{\beta}\sum_{\omega_n}\sum_{\mathbf{k}}e^{i\omega_n\tau}\int_0^{\tilde{J}_{s\text{-}f}}\frac{d\lambda}{\lambda}G(\mathbf{k},i\omega_n)\Sigma(\mathbf{k},i\omega_n)\ , \tag{3.1}$$

where $G(\mathbf{k},i\omega_n)$ denotes the temperature Green's function for the conduction electron with the wave vector $\mathbf{k}$. In paramagnetic phase, $G(\mathbf{k},i\omega_n)$ is independent of spin. Σ is its self-energy, which may be expressed as

$$\Sigma(\mathbf{k},i\omega_n)=\frac{\tilde{J}_{s\text{-}f}^2}{4N}\frac{1}{\beta}\sum_{\omega_m'}\sum_{\mathbf{k}'}\sum_{\mu=xyz}G(\mathbf{k}',i\omega_m')\times\mathrm{Tr}\hat{\chi}_f(\mathbf{k}-\mathbf{k}',i\omega_n-\omega_m'), \tag{3.2}$$

where $\hat{\chi}_f\equiv(\chi_f^{\mu\nu})$ $(\mu,\nu=x,y,z)$ is the dynamic susceptibility tensor for the f electrons in units of $(g_J\mu_B)^2$, defined as

$$\hat{\chi}_f(\mathbf{q},i\nu)=\sum_j e^{i\mathbf{q}\cdot\mathbf{R}_{ij}}\int_0^\beta d\tau\, e^{-\tau\nu}\langle \mathbf{J}_i(\tau)\cdot\mathbf{J}_j\rangle . \tag{3.3}$$

Diagrammatically (3.2) is represented as Fig. 1(a).

We calculate $\hat{\chi}_f$ by the bubble approximation (RPA) shown in Fig. 1(b). In the site representation, the right-hand side of Fig. 1(b) shows that χ_f consists of the Van Vleck susceptibility $\chi_f(0)^{\mu\nu}(\omega)$ at various sites and the unperturbed conduction susceptibility $\chi_c^{(0)}$ connecting these different sites. Thus χ_f expresses the propagation of magnetic excitation from site to site.

Here the case in which $\chi_c^{(0)}$ connects the same site is excluded.[13] The reason for this can be seen by the second-order perturbation calculation for $\hat{\chi}_f$. In order to make concrete understanding, we adopt a simplified model in which $J=1$ and the crystalline states are described by

$$H_{\mathrm{cry}}=\sum_i \Delta(J_i^z)^2 . \tag{3.4}$$

For the conduction band with the constant density of states per spin $N(0)$ and the band width $2D$, the susceptibility for different sites $(i\neq j)$ is calculated as

$$\chi_{fij}^{(2)}(\omega=0)=2\left[\frac{\tilde{J}_{s\text{-}f}}{N\Delta}\right]^2\sum_{\mathbf{k}\mathbf{k}'}\frac{f(\varepsilon_{\mathbf{k}'})-f(\varepsilon_{\mathbf{k}})}{\varepsilon_{\mathbf{k}'}-\varepsilon_{\mathbf{k}}}e^{i(\mathbf{k}-\mathbf{k}')\mathbf{R}_{ij}} . \tag{3.5}$$

This is proportional to $1/\Delta^2$ because of the square of the Van Vleck susceptibility at the different sites. On the other hand, the susceptibility for the same site is calculated as

$$\chi_{fii}^{(2)}(\omega=0)=\left[\frac{\tilde{J}_{s\text{-}f}}{N}\right]^2\sum_{\mathbf{k}\mathbf{k}'}\frac{f(\varepsilon_{\mathbf{k}})\{1-f(\varepsilon_{\mathbf{k}'})\}}{\Delta(\varepsilon_{\mathbf{k}'}-\varepsilon_{\mathbf{k}}+\Delta)(\varepsilon_{\mathbf{k}'}-\varepsilon_{\mathbf{k}}-\Delta)}\times\left[1+\frac{4\Delta}{\varepsilon_{\mathbf{k}'}-\varepsilon_{\mathbf{k}}+\Delta}-\frac{2\Delta}{\varepsilon_{\mathbf{k}'}-\varepsilon_{\mathbf{k}}-\Delta}\right]$$
$$\simeq-\left[\frac{\tilde{J}_{s\text{-}f}^2N(0)}{\Delta N}\right]\frac{N(0)}{N}\ln\left[\frac{2\Delta}{D}\right] . \tag{3.6}$$

This is the susceptibility showing the Kondo anomaly.[14] That is, at the same site the square of the Van Vleck susceptibility is replaced by the much weaker logarithmic term, so that apart from the Ruderman-Kittel-Kasuya-Yosida (RKKY) oscillatory factor in (3.5)

$$\frac{\chi_{fii}^{(2)}(0)}{\chi_{f,ij}^{(2)}(0)}\simeq\frac{\Delta N(0)}{2N}\ln\left[\frac{2\Delta}{D}\right]\ll 1 . \tag{3.7}$$

Thus the calculation from the same site is neglected.

With this restriction, $\hat{\chi}_f$ in RPA is given by

$$\hat{\chi}_f^{\mathrm{RPA}}(\mathbf{q},i\nu)=\frac{\hat{\chi}_f^{(0)}(i\nu)}{1-(\tilde{J}_{s\text{-}f}^2/N)\hat{\chi}_f^{(0)}(i\nu)\chi_e^{(0)}(\mathbf{q},i\nu)} . \tag{3.8}$$

Here, $\chi_e^{(0)}(\mathbf{q},i\nu)$ is the Fourier transformation of the conduction electron susceptibility subtracted the same site contribution,

$$\chi_e^{(0)}(\mathbf{q},i\nu)=\chi_c^{(0)}(\mathbf{q},i\nu)-\bar{\chi} , \tag{3.9a}$$

where

$$\chi_c^{(0)}(\mathbf{q},i\nu)=\frac{1}{2}\cdot\sum_{\mathbf{k}}\frac{f(\varepsilon_{\mathbf{k}+\mathbf{q}})-f(\varepsilon_{\mathbf{k}})}{i\nu-\varepsilon_{\mathbf{k}+\mathbf{q}}+\varepsilon_{\mathbf{k}}} , \tag{3.9b}$$

$$\bar{\chi}=\frac{1}{N}\sum_{\mathbf{q}}\chi_c^{(0)}(\mathbf{q},i\nu) , \tag{3.9c}$$

and q is restricted to the first Brillouin zone (BZ).

It is different to calculate the ladder term as shown in Fig. 1(c), since in the present problem the dotted line, which represents the unperturbed Van Vleck susceptibili-

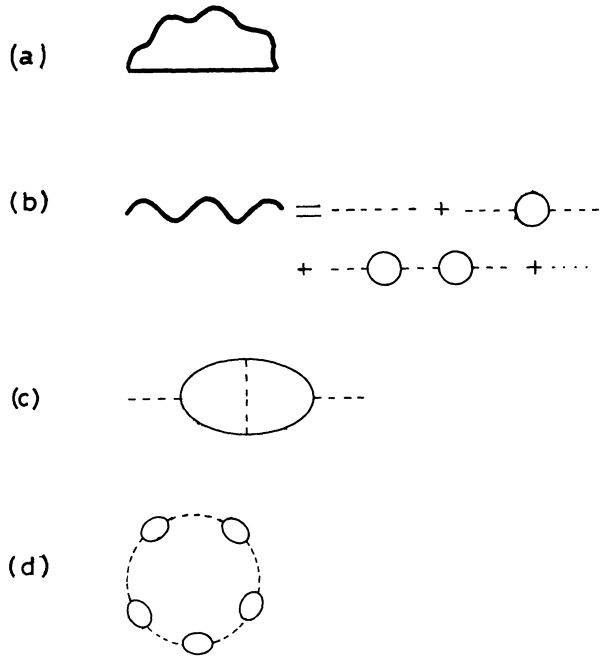

FIG. 1. Diagrams representing the following quantities: (a) the conduction electron self-energy, (b) the RPA f-electron susceptibility, (c) the lowest-order ladder term for the f-electron susceptibility, (d) the RPA thermodynamic potential. The light line represents $G_\sigma^{(0)}(\mathbf{k},i\omega)$, the bubble formed by it depicts the subtracted conduction electron susceptibility $\chi_e^{(0)}(\mathbf{q},i\nu)$, the heavy line for $G_\sigma(\mathbf{k},i\omega)$, the dashed line for $\chi_f^{(0)\mu\mu}(\mathbf{q},i\nu)$, and the wavy line for $\chi_f^{\mu\mu}(\mathbf{q},i\nu)$.

ty for the f electrons depends on ω, in contrast to the case of the Hubbard model, where the dotted line represents the ω independent interaction I. However, it has been shown in Ref. 8 that the contribution of the lowest-order ladder term of Fig. 1(c) for $\chi_f^{\mu\mu}(\mathbf{q},i\nu)$ is negligibly small at $q=0$ and $\omega=0$. Therefore, in Fig. 1(a) we replace the wavy line by the bubble type diagram.

Here one should note that the (μ,μ) component of $\chi_f^{\mathrm{RPA}}(\mathbf{q},i\nu)$ is expressed by $\chi_f^{(0)}(i\nu)$ with same μ. This is due to the bubble approximation. The simple replacement of I with (2.6) does not hold in (3.8). This reaches to all the calculation of this paper. Furthermore, in (3.1) and (3.2) we approximate the conduction electron Green's function by its unperturbed Green's function. Thus, as represented in Fig. 1(d), the RPA excess thermodynamic potential $\Delta\Omega$ is constituted as a set of bubbles expressing $\chi_e^{(0)}(\mathbf{q},i\nu)$ and dotted lines expressing $\chi_f^{(0)\mu\mu}(i\nu)$. It is given by

$$\Delta\Omega=\frac{1}{\beta}\sum_{\nu_n}\sum_{\mathbf{q}}\int_0^{\tilde{J}_{s\text{-}f}}d\lambda\chi_e^{(0)}(\mathbf{q},i\nu_n)\sum_{\mu}\frac{(\lambda/N)\chi_f^{(0)\mu\mu}(i\nu_n)}{1-(\lambda^2/N)\chi_f^{(0)\mu\mu}(i\nu_n)\chi_e^{(0)}(\mathbf{q},i\nu_n)}\ . \tag{3.10}$$

When a magnetic field is applied, we must use the diagonalized $\hat{\chi}_f^{(0)}$, as $\hat{\chi}_f^{(0)}$ is not diagonal. For $\chi_e^{(0)}(\mathbf{q},i\nu)$ neglecting its field dependence may be allowed. After performing the λ integration and the summation over ν_n, $\Delta\Omega$ is expressed as

$$\Delta\Omega=\sum_{\mathbf{q}\mu}\frac{\hbar}{2\pi}\int_{-\infty}^{\infty}\mathrm{Im}\ln\{1-(\tilde{J}_{s\text{-}f}^2/N)\chi_f^{(0)\mu\mu}(\omega+i\eta)\chi_e^{(0)}(\mathbf{q},\omega+i\eta)\}p(\hbar\omega)d\omega\ , \tag{3.11}$$

where $p(\hbar\omega)$ is the Planck distribution function, $p(\hbar\omega)=1/[\exp(\beta\hbar\omega)-1]$. Equation (3.11) can be obtained by replacing the interaction I with $(\tilde{J}_{s\text{-}f}^2/2N)\cdot\chi_f^{(0)\mu\mu}$ in the corresponding equation in Ref. 11.

The excess entropy ΔS can be obtained by differentiating (3.11) with T. However, the T derivative of $\chi_f^{(0)}$ can be neglected for temperatures much lower than the crystal-field splitting. As a result of this, it holds that

$$\begin{aligned}\Delta S&=-\frac{\partial}{\partial T}\Delta\Omega\\&=-\sum_{\mathbf{q}\mu}\frac{\hbar}{2\pi}\int_{-\infty}^{\infty}d\omega\frac{\partial}{\partial T}p(\hbar\omega)\mathrm{Im}\ln\left\{1-\frac{\tilde{J}_{s\text{-}f}^2}{N}\chi_f^{(0)\mu\mu}(\omega+i\eta)\chi_e^{(0)}(\mathbf{q},\omega+i\eta)\right\}\\&\quad+\sum_{\mathbf{q}\mu}\frac{\hbar}{2\pi}\int_{-\infty}^{\infty}d\omega\,p(\hbar\omega)\frac{(\tilde{J}_{s\text{-}f}^2/N)\chi_f^{(0)\mu\mu}(\omega+i\eta)(\partial/\partial T)\chi_e^{(0)}(\mathbf{q},\omega+i\eta)}{1-(\tilde{J}_{s\text{-}f}^2/N)\chi_f^{(0)\mu\mu}(\omega+i\eta)\chi_e^{(0)}(\mathbf{q},\omega+i\eta)}\ .\end{aligned} \tag{3.12}$$

Noting (3.9b), we derive the T derivative of the Fermi distribution function $f(\hbar\omega)$ from the second term of (3.12). After some calculation, we can obtain

$$\begin{aligned}\Delta S=-\sum_{\mathbf{q}\mu}\frac{\hbar}{2\pi}\int_{-\infty}^{\infty}d\omega\frac{\partial p(\hbar\omega)}{\partial T}&\left[\mathrm{Im}\ln\left\{1-\frac{\tilde{J}_{s\text{-}f}^2}{N}\chi_f^{(0)\mu\mu}(\omega+i\eta)\chi_e^{(0)}(\mathbf{q},\omega+i\eta)\right\}\right.\\&\left.+\frac{\tilde{J}_{s\text{-}f}^2}{N}\mathrm{Im}\chi_e^{(0)}(\mathbf{q},\omega+i\eta)\mathrm{Re}\chi_f^{\mathrm{RPA}\,\mu\mu}(\mathbf{q},\omega+i\eta)\right]-\sum_{\mathbf{k}\sigma}\frac{\partial}{\partial T}f(\varepsilon_{\mathbf{k}})\mathrm{Re}\Sigma^{\mathrm{RPA}}(\mathbf{k},\varepsilon_{\mathbf{k}})\ ,\end{aligned} \tag{3.13}$$

where

$$\mathrm{Re}\Sigma^{\mathrm{RPA}}(\mathbf{k},\varepsilon_{\mathbf{k}})=-\frac{\tilde{J}_{s\text{-}f}^2}{4N}\sum_{\mathbf{q}\mu}\int_{-\infty}^{\infty}\frac{\hbar\,d\omega}{\pi}\mathrm{Im}\chi_f^{\mathrm{RPA}\,\mu\mu}(\mathbf{q},\omega+i\eta)\ . \tag{3.14}$$

Equation (3.13) with (3.14) corresponds completely to the result of Brinkman and Engelsberg,[11] their Eq. (2.28) with (2.29). This parallelism comes from the following facts. First, we have limited ourselves in low temperatures so as to regard the Van Vleck susceptibility $\hat{\chi}_f$ as a T-independent constant. Secondly, we have collected only bubble terms. As a result of these, $J_{s\text{-}f}^2\chi_f^{\mu\mu}(\omega)/2N$ plays the same role as the interaction strength I in the Hubbard model. The difference of entropy between the Hubbard model and the present system appears through $\hat{\chi}_f(\omega)$, which is studied in the following sections. Brinkman and Engelsberg[11] called the first term in (3.13), which is proportional to the T-derivative of the Planck distribution function $p(\hbar\omega)$, a bosonlike term and denoted it as ΔS_B. Similarly the second term proportional to the T derivative of the Fermi distribution function was called as a fermionlike term and denoted as ΔS_F. Fulde and Jensen[4] have only considered the contribution of ΔS_F. We study ΔS_F and ΔS_B separately in the following subsections.

A. Fermionlike contribution

Separating real and imaginary parts of ΔS_F, we obtain

$$\Delta S_F=-\frac{\tilde{J}_{s\text{-}f}^2 N(0)^2}{2NT}\int_{-D}^{D}d\varepsilon\,\varepsilon\frac{\partial}{\partial\varepsilon}f(\varepsilon)\int_{-D}^{D}d\varepsilon'\sum_{\mu}\left[\frac{\hbar}{\pi}\int_{-\infty}^{\infty}p(\hbar\omega)\mathrm{Im}\bar{\chi}_f^{\mathrm{RPA}\,\mu\mu}(\omega+i\eta)\frac{P}{\varepsilon-\varepsilon'-\omega}d\omega\right.$$
$$\left.-[1-f(\varepsilon')]\mathrm{Re}\bar{\chi}_f^{\mathrm{RPA}\,\mu\mu}(\varepsilon-\varepsilon')\right], \tag{3.15}$$

with

$$\bar{\chi}_f^{\mathrm{RPA}\,\mu\mu}(\omega+i\eta)=\frac{1}{2k_F^2}\int_0^{2k_F}dq\,q\chi_f^{\mathrm{RPA}\,\mu\mu}(\mathbf{q},\omega+i\eta)\,. \tag{3.16}$$

In deriving (3.15), we have assumed a constant density of states for the conduction electrons. D and $N(0)$ denote a half of the conduction band width and its density of states per spin, respectively. As the principal part integral appearing in (3.15) only gives a value of the order of $1/D$, we can neglect this term. From (3.15) the excess specific heat ΔC_F coming from ΔS_F is expressed as

$$\Delta C_F=T\frac{\partial}{\partial T}(\Delta S_F)$$
$$=T\frac{\tilde{J}_{s\text{-}f}^2 N(0)^2}{2N}\sum_{\mu}\int_{-D}^{D}d\varepsilon\int_{-D}^{D}d\varepsilon'\left\{-\frac{\varepsilon}{T}\frac{\partial f(\varepsilon)}{\partial\varepsilon}\frac{\varepsilon'}{T}\frac{\partial f(\varepsilon')}{\partial\varepsilon'}\mathrm{Re}\bar{\chi}_f^{\mathrm{RPA}\,\mu\mu}(\varepsilon-\varepsilon')\right.$$
$$\left.+\left[\frac{\varepsilon}{T^2}\frac{\partial f(\varepsilon)}{\partial\varepsilon}+\frac{\varepsilon}{T}\frac{\partial}{\partial\varepsilon}\left[\frac{\varepsilon}{T}\frac{\partial f(\varepsilon)}{\partial\varepsilon}\right]\right][1-f(\varepsilon')]\mathrm{Re}\bar{\chi}_f^{\mathrm{RPA}\,\mu\mu}(\varepsilon-\varepsilon')\right\}. \tag{3.17}$$

Integrating (3.17) over ε partially, we obtain

$$\Delta C_F=\frac{\tilde{J}_{s\text{-}f}^2 N(0)^2}{4TN}\sum_{\mu}\int_{-D}^{D}d\varepsilon\int_{-D}^{D}d\varepsilon'(\varepsilon-\varepsilon')^2\frac{\partial f(\varepsilon)}{\partial\varepsilon}\frac{\partial f(\varepsilon')}{\partial\varepsilon'}\mathrm{Re}\bar{\chi}_f^{\mathrm{RPA}\,\mu\mu}(\varepsilon-\varepsilon')\,. \tag{3.18}$$

First we calculate (3.18) in the low-temperature expansion. In the free-electron model, $\chi_e^{(0)}(\mathbf{q},\omega)$, which is through (3.8) and (3.16) the constituent of $\bar{\chi}_f^{\mathrm{RPA}}$ in (3.18), is expressed by $N(0)L(q,\omega)/2$, where $N(0)$ is, in this case, the density of states per spin at E_F and $L(q,\omega)$ is the effective Lindhard function subtracted $\bar{\chi}$ from the Lindhard function. Because of the ε derivative of the Fermi distribution function in (3.18), a contribution from the region of q and ω satisfying $\hbar\omega\ll E_F$, $q\ll k_F$, and $\omega\ll v_F\cdot q$ is dominant to the specific heat. In this region $L(q,\omega)$ is expressed as

$$L(q,\omega)=\delta-\frac{\tilde{q}^2}{3}-\frac{\tilde{\omega}^2}{\tilde{q}^2}+i\frac{\pi\tilde{\omega}}{2\tilde{q}}+\cdots\,, \tag{3.19}$$

where $\delta=1-2\bar{\chi}/N(0)$, $\tilde{q}=q/2k_F$, and $\tilde{\omega}=\omega/(2k_Fv_F)$. We have neglected here the temperature dependence of $L(q,\omega)$. Substituting (3.19) in (3.8) and expanding it, we obtain

$$\mathrm{Re}\chi_f^{\mathrm{RPA}\,\mu\mu}(\mathbf{q},\omega)=\frac{\chi_f^{(0)\mu\mu}(0)}{1-\alpha^\mu(0)(\delta-\tilde{q}^2/3)}-\frac{\alpha^\mu(0)\chi_f^{(0)\mu\mu}(0)}{\{1-\alpha^\mu(0)(\delta-\tilde{q}^2/3)\}^2}\frac{\tilde{\omega}^2}{\tilde{q}^2}$$
$$-\frac{(\pi/4)[\alpha^\mu(0)]^2\chi_f^{(0)\mu\mu}(0)}{\{1-\alpha^\mu(0)(\delta-\tilde{q}^2/3)\}^3}\frac{\tilde{\omega}^2}{\tilde{q}^2}+\frac{\frac{1}{2}(\partial^2/\partial^2\omega)\chi_f^{(0)\mu\mu}(0)}{\{1-\alpha^\mu(0)(\delta-\tilde{q}^2/3)\}^2}\omega^2+\cdots\,, \tag{3.20}$$

where

$$\alpha^\mu(\omega)=[\tilde{J}_{s\text{-}f}^2/2N]N(0)\chi_f^{(0)\mu\mu}(\omega)\,, \tag{3.21}$$

which is a correspondent of $IN(0)$ in the Hubbard model.

In (3.15), the last term coming from the ω derivative of $\alpha^\mu(\omega)$ gives a new aspect of the present system in contrast with the Hubbard model. This represents the effect of time dependence of the effective interaction. As for the second and third terms, they are both proportional to $(\tilde{\omega}/\tilde{q})^2$. However, the second term can be neglected compared with the third term by the factor $[1-\alpha^\mu(0)(\delta-\tilde{q}^2/3)]^{-1}$, as we are interested in the case of large amount of this enhancement factor.

Inserting the remaining terms in (3.20) into (3.18), we obtain

$$\Delta C_F=\frac{N(0)}{2T}\sum_{\mu}\int_{-D}^{D}d\varepsilon\int_{-D}^{D}d\varepsilon'(\varepsilon-\varepsilon')^2\frac{\partial f(\varepsilon)}{\partial\varepsilon}\frac{\partial f(\varepsilon')}{\partial\varepsilon'}\{\bar{\alpha}_1^\mu(\varepsilon-\varepsilon')+\bar{\alpha}_2^\mu(\varepsilon-\varepsilon')+\bar{\alpha}_3^\mu(\varepsilon-\varepsilon')+\cdots\}\,, \tag{3.22}$$

$$\bar{\alpha}_1^{\mu}(\omega)\equiv 2\int_0^1 d\tilde{q}\,\tilde{q}\frac{\alpha^{\mu}(0)}{1-\alpha^{\mu}(0)(\delta-\tilde{q}^2/3)},$$

$$\bar{\alpha}_2^{\mu}(\omega)\equiv 2\int_{\tilde{q}_0}^1 d\tilde{q}\,\tilde{q}\frac{(\pi^2/8)[\alpha^{\mu}(0)]^3}{\{1-\alpha^{\mu}(0)(\delta-\tilde{q}^2/3)\}^3}\frac{\tilde{\omega}^2}{\tilde{q}^2}, \tag{3.23}$$

$$\bar{\alpha}_3^{\mu}(\omega)\equiv 2\int_0^1 d\tilde{q}\,\tilde{q}\frac{\frac{1}{2}(\partial^2/\partial\varepsilon^2)\alpha^{\mu}(0)\omega^2}{\{1-\alpha^{\mu}(0)(\delta-\tilde{q}^2/3)\}^2},$$

where q_0 is the lower limit to assign the region for the imaginary part in (3.19). As the series expansion of $L(q,\omega)$ in (3.19) does not hold in $\tilde{\omega}\geq\tilde{q}$, we can take $\tilde{q}_0$ as $\tilde{\omega}$. On the other hand, as the integrands for α_1,α_3 are regular at $q=0$, we can replace $\tilde{q}_0$ with 0. By changing the variable $\tilde{q}$ to $x\equiv\tilde{q}^2$, (3.23) is integrated as

$$\bar{\alpha}_1^{\mu}(\omega)=3\ln\left[1+\frac{1}{3}\frac{\alpha^{\mu}(0)}{1-\delta\alpha^{\mu}(0)}\right],$$

$$\bar{\alpha}_2^{\mu}(\omega)=-\frac{\pi^2}{4}\left[\frac{\alpha^{\mu}(0)}{1-\delta\alpha^{\mu}(0)}\right]^3\tilde{\omega}^2\ln|\tilde{\omega}|, \tag{3.24}$$

$$\bar{\alpha}_3^{\mu}(\omega)=\frac{\frac{1}{2}(\partial^2/\partial\varepsilon^2)\alpha^{\mu}(0)\omega^2}{[1-\delta\alpha^{\mu}(0)][1+(\frac{1}{3}-\delta)\alpha^{\mu}(0)]}.$$

Substituting (3.22) into (3.24), we obtain

$$\Delta C_F=\frac{3}{2}\sum_{\mu=xyz}\ln\left[1+\frac{1}{3}\frac{\alpha^{\mu}(0)}{1-\delta\alpha^{\mu}(0)}\right]\gamma_0 T+\frac{3\pi^2}{80}\gamma_0 T\left[\frac{T}{T_F}\right]^2\ln\left[\frac{T}{4T_F}\right]\sum_{\mu}\left[\frac{\alpha^{\mu}(0)}{1-\delta\alpha^{\mu}(0)}\right]^3+\frac{36\pi^2}{5}\gamma_0 T\sum_{\mu}\left[\frac{k_B T}{\Delta^{\mu}}\right]^2+\cdots, \tag{3.25}$$

with

$$\gamma_0=\tfrac{2}{3}\pi^2 k_B^2 N(0),$$
$$\Delta^{\mu}=\hbar\cdot\left[\frac{1-\delta\alpha^{\mu}(0)}{\frac{1}{2}(\partial^2/\partial\omega^2)\alpha^{\mu}(0)}\right]^{1/2}. \tag{3.26}$$

The above result (3.25) was reported in a previous paper[9] without giving derivation.

The first term in (3.25) is the T-linear specific heat with mass enhancement

$$\frac{m^*}{m}-1=\frac{3}{2}\sum_{\mu=xyz}\ln\left[1+\frac{1}{3}\frac{\alpha^{\mu}(0)}{1-\delta\alpha^{\mu}(0)}\right]. \tag{3.27}$$

The second term is the correction to the T-linear term. These T and $T^3\ln T$ terms correspond to those in the Hubbard model[10] when the ω dependence of the Van Vleck susceptibility is neglected. On the other hand, the third term, which is proportional to T^3, manifests this ω dependence, as can be seen from (3.26). Since $[\partial^2\alpha^{\mu}(0)/\partial\omega^2]/\hbar^2\simeq\alpha^{\mu}(0)/(E_{N0})^2$ and $\delta\alpha^{\mu}(0)\simeq 1$ in the present system, Δ^{μ} amounts to a fraction of the crystal-field splitting. The T^3 term normalized by Δ^{μ} is therefore predominant than the $T^3\ln T$ term to correct the T-linear term. All the terms in (3.25) depend on the enhancement factor $[1-\delta\alpha^{\mu}(0)]^{-1}$. Thus the higher-order terms in (3.25) may become important depending on the value of $\alpha^{\mu}(0)$ and T.

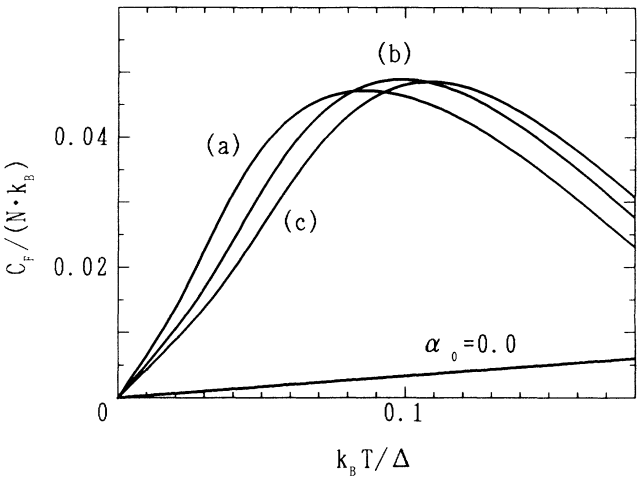

FIG. 2. Specific heat of the fermionic term for the model (3.4) as a function of temperature for several values of α_0. The solid lines represent C_F/Nk_B and (a), (b), and (c) correspond to the cases at $\delta\alpha_0=0.95$, 0.9, and 0.85, respectively.

Up to here we have studied the low-temperature expansion of C_F. To examine the contributions of the higher-order terms, we calculate numerically C_F for the model introduced in (3.4). It holds that $\alpha^x(0)=\alpha^y(0)\equiv\alpha_0$, $\alpha^z(0)=0$. In the Appendix we describe the calculation of the susceptibility for (3.4) in the presence of applied field. Calculating (3.18) and (A4) at $h=0$ numerically, we obtained C_F/Nk_B. The results for $\Delta N(0)=0.005$ are shown in Fig. 2 by solid lines. Following feature can be seen in this figure. When $\delta\alpha_0$ is nearly unity, corresponding to the Doniach-Engelsberg theory the linear coefficient of C_F is highly enhanced. By the higher-order effect of $I(\omega)$, with increase of temperature C_F deviates upward from the T-linear behavior and after passing the maximum C_F goes down. As $\delta\alpha_0$ approaches unity, the peak of C_F shifts to the low-temperature side.

B. Bosonlike contribution

Next we study a contribution of the bosonlike term defined in (3.13), which can be written as

$$\Delta S_B=\sum_{\mathbf{q}\mu}\frac{\hbar}{2\pi}\int_{-\infty}^{\infty}d\omega\frac{\partial p(\hbar\omega)}{\partial T}\left\{\arctan^{\mu}(\mathbf{q},\omega)-\frac{\tilde{J}_{s\text{-}f}^2}{N}\mathrm{Re}\chi_f^{\mathrm{RPA}\mu\mu}(\mathbf{q},\omega+i\eta)\mathrm{Im}\chi_e^{(0)}(\mathbf{q},\omega+i\eta)\right\}, \tag{3.28}$$

where

$$g^{\mu}(\mathbf{q},\omega)=\frac{(\tilde{J}_{s\text{-}f}^2/N)\chi_f^{(0)\mu\mu}(\omega)\mathrm{Im}\chi_e^{(0)}(\mathbf{q},\omega+i\eta)}{1-(\tilde{J}_{s\text{-}f}^2/N)\chi_f^{(0)\mu\mu}(\omega)\mathrm{Re}\chi_e^{(0)}(\mathbf{q},\omega+i\eta)} . \tag{3.29}$$

Strong ω dependence of $g^{\mu}(\mathbf{q},\omega)$ ($\mu=x,y,z$) comes from $\chi_f^{(0)\mu\mu}(\omega)$ expressed in (2.4), which is singular at the crystal-field splitting energies $\hbar\omega=E_n-E_g\equiv E_{ng}^{(0)\mu}$ (n indicates excited states), approximately several tens of K. In (3.29) we have had to neglect the imaginary part of $\chi_f^{(0)\mu\mu}(\omega+i\eta)$ appearing in (3.13) as its singularity due to the δ function appears both in the numerator and the denominator of (3.29), and they cancel each other. When we move ω from the lower energy, $\chi_f^{(0)\mu\mu}(\omega)$ increases and the denominator in (3.29) turns negative after taking zero. This zero point is denoted as $E_{ng}^{\mu}(q)$ corresponding to $E_{ng}^{(0)\mu}$ the singular point of $\chi_f^{(0)\mu\mu}(\omega)$. Each $E_{ng}^{\mu}(q)$ is slightly smaller than $E_{ng}^{(0)\mu}$, because $\tilde{J}_{s\text{-}f}=0.1$–$0.01$ eV and $\mathrm{Re}\chi_e^{(0)}(\mathbf{q},\omega+i\eta)/N\sim 0(1/E_F)$. It is clear from (3.29) that $\mathrm{arctang}^{\mu}(\mathbf{q},\omega)$ is equal to $\pi/2$ at $\hbar\omega=E_{ng}^{\mu}$ and increases up to π when ω approaches $E_{ng}^{(0)\mu}$. After passing $E_{ng}^{(0)\mu}$ the denominator of (3.29) turns positive and the numerator turns negative. Hence, $\mathrm{arctang}^{\mu}(\mathbf{q},\omega)$ suddenly changes from π to negative value. If we notice that $\mathrm{Re}\chi_e^{(0)}(\mathbf{q},\dot{\omega}+i\eta)/N\sim 0(1/E_F)$ and $\mathrm{Im}\chi_e^{(0)}(\mathbf{q},\omega+i\eta)/N\sim N(0)\omega/v_F q\sim 0(E_{ng}^{(0)\mu}/E_F^2)$ for ω of the order $E_{ng}^{(0)\mu}$, and $\tilde{J}_{s\text{-}f}/E_F\ll 1$, it turns out that the most change of (3.29) occurs in the neighborhood of narrow region $[E_{ng}^{\mu}(q), E_{ng}^{(0)\mu}]$. On the other hand, outside this narrow region, it turns out from the above-mentioned facts for $\chi_e^{(0)}(\mathbf{q},\omega+i\eta)$ and $\tilde{J}_{s\text{-}f}$ that $g^{\mu}(\mathbf{q},\omega)$ takes a small value, so that $\mathrm{arctang}^{\mu}(\mathbf{q},\omega)$ is well approximated there with $g^{\mu}(\mathbf{q},\omega)$. After all, these observations allow us as the lowest approximation to write

$$\mathrm{arctang}^{\mu}(\mathbf{q},\omega)=g^{\mu}(\mathbf{q},\omega)+\pi\sum_n[\theta(\hbar\omega-E_{ng}^{\mu}(q))-\theta(\hbar\omega-E_{ng}^{(0)\mu})] , \tag{3.30}$$

where $\theta(\hbar\omega)$ is the step function.

We consider here the second term in the parenthesis of (3.28). If we notice in the expression of $\mathrm{Re}\chi_f^{\mathrm{RPA}}(\mathbf{q},\omega+i\eta)$ derived from (3.8) that the part consisting of $\mathrm{Im}\chi_e^{(0)}(\mathbf{q},\omega+i\eta)$ is negligibly small compared with the remaining parts by the same reason as mentioned above, the second term of (3.28) can be approximated by $-g^{\mu}(\mathbf{q},\omega)$. Then (3.28) with (3.30) is reduced to

$$\Delta S_B=\sum_{\mathbf{q}\mu}\frac{\hbar}{2\pi}\int_0^{\infty}d\omega\frac{\partial}{\partial T}p(\hbar\omega)\sum_n[\theta(\hbar\omega-E_{ng}^{\mu}(q))-\theta(\hbar\omega-E_{ng}^{(0)\mu})] . \tag{3.31}$$

From (3.31) we can easily derive the expression for the specific heat from the bosonlike term

$$\Delta C_B=\sum_{\mathbf{q}\mu}\sum_n\left[\frac{\partial}{\partial T}p[E_{ng}^{\mu}(q)]E_{ng}^{\mu}(q)-\frac{\partial}{\partial T}p(E_{ng}^{(0)\mu})E_{ng}^{(0)\mu}\right] . \tag{3.32}$$

This result tells a simple interpretation for the bosonlike contribution and clarifies the meaning of the approximation made above. Since $E_{ng}^{\mu}(q)$ is defined as the zero point of the denominator of (3.29), it is the pole of $\chi_f^{\mathrm{RPA}\,\mu\mu}(\mathbf{q},\omega+i\eta)$ in (3.8) when its imaginary part is neglected. Therefore, the first term in the parenthesis of (3.32) is the specific heat of the magnetic excitation and the present approximation is to neglect the effect of its life time. The spectrum of this magnetic excitation is caused by the transfer of the excitation of the singlet ground state by the conduction electron polarization (the RKKY mechanism). There exists a gap for each mode μ otherwise the system cannot remain in the paramagnetic state. The second term in (3.32) cancels out the contribution of the noninteracting Van Vleck ions, which is included in the unperturbed term.

The magnetic excitation energy is given by the pole of $\chi_f^{\mathrm{RPA}}(\mathbf{q},\omega)$ in (3.8). For the free electron band $\chi_e^{(0)}(\mathbf{q},\omega)$ is expressed by the effective Lindhard function $L(q,\omega)$. Using $\alpha^{\mu}(\omega)$ defined in (3.21), we rewrite the denominator of (3.8) as

$$1-\alpha^{\mu}(\omega)L(q,\omega)=0 . \tag{3.33}$$

We notice that the ω dependence of $L(q,\omega)$ can be neglected compared with that of $\alpha^{\mu}(\omega)$ in (3.33), since in the former ω is normalized by E_F, whereas in the latter ω is normalized by the crystal-field splitting energy. In this procedure the imaginary part of $L(q,\omega)$ expressed in (3.19), namely, the lifetime effect, is also neglected.

For the model defined in (3.4) we calculate numerically the dispersion relation of the magnetic excitations. From (A3) the results are shown in Fig. 3 for several values of $\delta\alpha_0$, when $h=0$. As the excited states for (3.4) are doublet, the excitation modes $E^x(q)$ and $E^y(q)$ are degenerate. The excitation mode $E^z(q)$ does not exist, because $\chi_f^{zz}(\omega)=0$. The straight line in Fig. 3 denotes the crystal-field excitation energy of a noninteracting Van Vleck ion. The magnetic excitations are propagated by the RKKY mechanism and the discrete energy levels of the crystal-field states turn into a band. When $\delta\alpha_0$ approaches unity, a gap of the magnetic excitation turns small as is shown in Fig. 3.

As the second term in (3.32) and the unperturbed specific heat of the crystal-field states are negligible in low temperatures, the bosonlike contribution is written as

$$C_B=\sum_{\mu}\left[\frac{V}{2\pi^2}\int_0^{q_{\max}}dq\,q^2E^{\mu}(q)\frac{\partial}{\partial T}p(E^{\mu}(q))\right] , \tag{3.34}$$

where a cutoff $q_{\max}$ is introduced in place of the first BZ sum and V is the volume of the system.

Finally we calculate the effect of magnetic field for the electronic specific heat in the crystal-field model (3.4). For a magnetic field applied along the z axis the doublet excited states are lineally split by Zeeman effect. For a magnetic field applied along the x axis, the energy split-

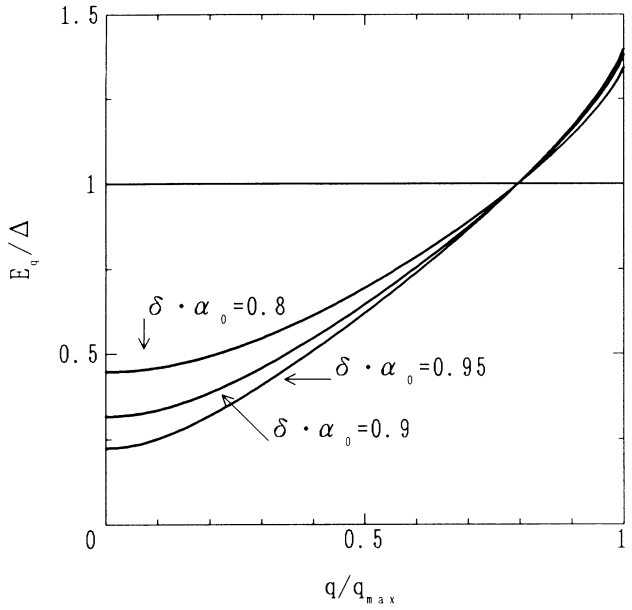

FIG. 3. Dispersion relation of magnetic excitons for the model (3.4). The dispersion curve is common for the polarization modes E_x/Δ and E_y/Δ defined in (3.33). The upper straight line shows the crystal-field energy splitting.

ting between the symmetric state $|s\rangle=(|1\rangle+|-1\rangle)/\sqrt{2}$ and the ground state $|0\rangle$ spreads. The antisymmetric state $|a\rangle=(|1\rangle-|-1\rangle)/\sqrt{2}$ does not vary. In this model the direction of the applied field produces the different effects.

Figure 4 is for the field applied along the z and x axes. Dashed lines indicate C_F/Nk_B and solid lines indicate

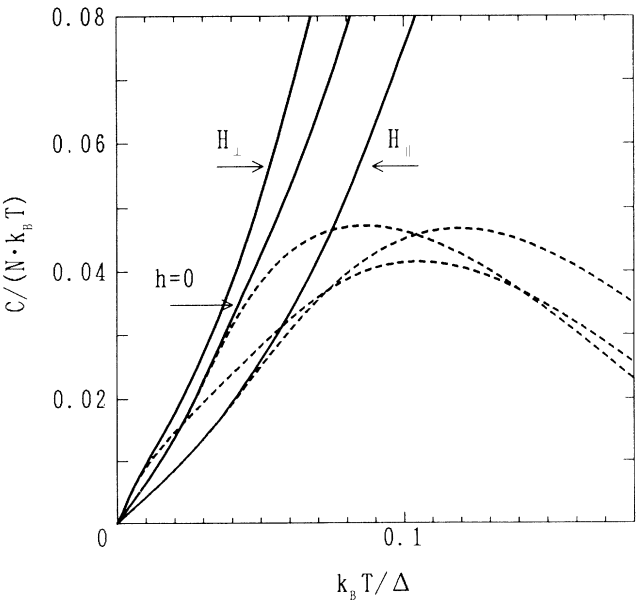

FIG. 4. Electronic specific heat of the model (3.4) as a function of temperature for magnetic fields $H_\parallel$ and $H_\perp$ applied along the z and x axis, respectively. Field strength is $h/\Delta=0.2$ in both cases. The dashed line represents C_F and the solid line represents the sum of C_F and C_B.

$(C_F+C_B)/Nk_B$ at $\Delta N(0)=0.005$. We have put $q_{max}=2k_F$ introduced in (3.34). When the field is applied along the z axis, one can see from the line $(H_\parallel)$ that with increasing field the slope of the T-linear specific heat increases. This is because $\delta\alpha_0$ approaches unity with decreasing energy splitting between $|0\rangle$ and $|1\rangle$. On the other hand, when the field is applied in the xy plane, C_F behaves oppositely to the above case. It is shown by the line $(H_\perp)$ by the dashed line. In these cases the width of the hill of C_F spreads with increasing field, since the doublet excited states are split with the magnetic field. C_B is negligibly small at low temperatures. With increasing temperature, C_B becomes dominant and tends to cover the deviation of C_F from the T-linear behavior.

IV. SUMMARY AND DISCUSSION

In this paper we have studied the effect of the electron-electron interaction mediated by the virtual excitation of the singlet ground state on the electronic specific heat. It has been shown in the previous work[8] that this effective interaction is repulsive for the electrons near the Fermi surface but turns attractive above the crystal-field splitting. If the effective interaction were repulsive, irrespective of ω, the specific heat would be given by the Doniach-Engelsberg-Brinkman theory[10,11] in any temperatures. Our study began by inquiring to what extent the specific heat resembles that of the Hubbard model and differs from it.

The specific heat has been derived from T-derivative of the thermodynamic potential. Following Brinkman and Engelsberg[11] we have separated the specific heat into the fermionlike contribution and the bosonlike contribution. The former stems from the particle-hole pair excitation of conduction electrons. The T-linear part corresponds exactly to that in the Hubbard model. Enhancement of the effective mass is given by the expression in the Hubbard model with the effective repulsive interaction at the Fermi surface. However, the $T^3\ln T$ term characteristic to the Doniach-Engelsberg theory is covered by T^3 term. Although this contribution has weaker T dependence than $T^3\ln T$ term, T is here normalized by the crystal-field splitting in place of E_F. The T^3 term is a sign of the finite level splitting or the ω dependence of the effective interaction. At high temperatures correspondence with the Hubbard model no longer holds.

As for the bosonlike contribution, we have derived the specific heat of the collective excitation modes directly from the s-f exchange interaction, which corrects the Schottky specific heat of individual Van Vleck ions. When we have calculated this magnetic excitation, we have neglected its imaginary part. This is because the damping due to electron-hole pair excitation is negligible in the degenerate electron gas. As far as the system remains paramagnetic, this magnetic excitation spectrum has a finite gap. It begins to work at temperatures comparable to the gap.

We have calculated numerically the specific heat for the simplified model to see the relative size of the fermionlike and bosonlike contributions in the presence of the magnetic field. Field dependence of the specific heat

plays a role to select the present mechanism out of others. In our model, the crystal-field states behave in different ways depending on the field direction. For a field parallel to the z axis the energy splitting of the crystal-field states decreases with increasing field. Then the strength of effective electron-electron interaction increases and so does the slope γ of the T-linear term. However, with increasing γ departure from the T-linear behavior shifts to the lower temperature side. For a field in the xy plane the energy splitting spreads with field so that the T-linear behavior holds up to high temperatures. However, the numerical calculation shows that the bosonlike contribution covers the fermionlike contribution in higher temperatures. Because of this the deviation from the T-linear behavior does not appear explicitly.

The Pr metal has a double-hexagonal closed packed structure. Pr ions at the hexagonal site are more effective than those at the cubic sites to the specific heat with excited states of smaller energy splitting.[4,15] The lower states of the hexagonal site are $|0\rangle$ and $|\pm 1\rangle$. In this sense our model roughly simplifies it and gives qualitative understanding for it. Then z axis and xy plane, respectively, correspond to c axis and to basal plane in our model. In the case of the field applied in the basal plane, behavior such as Fig. 4 is seen in the experimental results by Forgan,[5] and is consistent with the theoretical results by White-Fulde[3] and Fulde-Jensen.[4] For the field applied along the c axis, we therefore expect a field dependence similar to Fig. 4. However, at low temperatures and in a magnetic field, a contribution of nuclear spins for specific heat turns dominant. Then in the lower temperature region the T-linear specific heat of C_F is covered again.

Takayanagi *et al.*[16] found experimentally in $PrCu_6$ that the T-linear specific heat is twice as large as that of $LaCu_6$. To clarify whether this is due to the present mechanism, it is hoped to measure its field dependence.

To study the effect of the electron-electron interaction mediated by the virtual excitation of the singlet ground state, microscopic probes might be useful. It is known that the nuclear relaxation rate T_1^{-1} is enhanced by the repulsive electron-electron interaction.[17] In parallel with this theory we have pointed out the possibility of the enhancement of T_1^{-1} by the present mechanism.[7,9] It seems interesting to investigate other quantities influenced by the present mechanism, including the hyperfine-enhanced nuclear magnetism.

APPENDIX

We calculate here the f electron susceptibility defined in (3.8) and the dispersion relation of magnetic excitons for the model given by (3.4) with $J=1$. We consider two different cases depending on the applied field direction.

(i) When a magnetic field is applied along the z axis, the Hamiltonian (3.4) is rewritten as

$$H_{\rm cry}=\sum_i \Delta (J_i^z)^2+\sum_i hJ_i^z \ , \tag{A1}$$

where $h\equiv g_j\mu_B H$. From (2.4) and (A1), $\hat{\chi}_f^{(0)}(\omega)$ is immediately obtained as

$$\hat{\chi}_f^{(0)}(\omega)\equiv \begin{bmatrix} \chi_f^{(0)xx} & \chi_f^{(0)xy} & \chi_f^{(0)xy} \\ \chi_f^{(0)yx} & \chi_f^{(0)yy} & \chi_f^{(0)yz} \\ \chi_f^{(0)zx} & \chi_f^{(0)zy} & \chi_f^{(0)zz} \end{bmatrix}$$

$$= \begin{bmatrix} & & 0 \\ & \hat{\chi}_2^{(0)}(\omega) & 0 \\ 0 & 0 & 0 \end{bmatrix} , \tag{A2a}$$

$$\hat{\chi}_2^{(0)}(\omega)=\left[\frac{\Delta_+}{\Delta_+^2-\omega^2}+\frac{\Delta_-}{\Delta_-^2-\omega^2}\right]1$$

$$-\left[\frac{\omega}{\Delta_+^2-\omega^2}+\frac{\omega}{\Delta_-^2-\omega^2}\right]\sigma_y \ , \tag{A2b}$$

where $\Delta_\pm=\Delta\pm h$. Operating the unitary transform which diagonalizes (A2a) on (3.8) and making its trace, we obtain

$$\frac{\tilde{J}_{\rm sf}^2}{2N}N(0){\rm Tr}\hat{\chi}_f^{\rm RPA}(\mathbf{q},\omega)=\frac{\Delta\alpha_0^2}{2\sqrt{1-\alpha_0 L(q,0)}}\left[\frac{1}{E_+(q)-\omega}+\frac{1}{E_+(q)+\omega}+\frac{1}{E_-(q)-\omega}+\frac{1}{E_-(q)+\omega}\right] , \tag{A3a}$$

where

$$E_\pm(q)=\pm h+\Delta\sqrt{1-\alpha_0 L(q,0)} \ . \tag{A3b}$$

(ii) When a magnetic field is applied along the x axis, the Zeeman term $J_i^z h$ is replaced with $J_i^x h$ in (A1). From (2.4), $\hat{\chi}_f$ is obtained as

$$\hat{\chi}_f^{(0)}(\omega)\equiv \begin{bmatrix} \dfrac{2\Delta^3}{\Delta^2+4h^2}\dfrac{1}{(\Delta^2+4h^2)-\omega^2} & 0 & 0 \\ 0 & & \\ 0 & & \hat{\chi}_2^{(0)}(\omega) \end{bmatrix} , \tag{A4a}$$

where

$$\hat{\chi}_2^{(0)}(\omega)=\frac{\Delta_a^2-h^2}{\Delta_s}\frac{1}{\Delta_a^2-\omega^2}\mathbf{1} - \frac{2h}{\Delta_s}\frac{\omega}{\Delta_a^2-\omega^2}\sigma_y+\frac{\Delta_a}{\Delta_a^2-\omega^2}\sigma_z \ , \qquad \Delta_s=\sqrt{\Delta^2+4h^2}, \quad \Delta_a=\frac{\Delta+\sqrt{\Delta^2+4h^2}}{2} \ , \tag{A4b}$$

where Δ_a is the energy difference between $|a\rangle$ and a ground state. Δ_s is the energy interval between another excited state, which turns into $|s\rangle$ at $h=0$:

$$\frac{\tilde{J}_{sf}^2}{2N}N(0)\mathrm{Tr}\hat{\chi}_f^{\mathrm{RPA}}(\mathbf{q},\omega) = \sum_{\eta=s\pm,a}\frac{M_\eta(q)}{2}\left[\frac{1}{E_\eta(q)-\omega}+\frac{1}{E_\eta(q)+\omega}\right] , \tag{A5}$$

where

$$E_{s\pm}(q)=[A_2(q)\pm\sqrt{(A_2(q))^2-A_1(q)}]^{1/2} \ , \qquad E_a(q)=\left[\Delta_s^2-\frac{\alpha_0\Delta^4}{\Delta_s^2}L(q,0)\right]^{1/2} \ , \tag{A6}$$

$$M_{s\pm}(q)=\frac{\pm\Delta}{\{E_{s+}(q)\}^2-\{E_{s-}(q)\}^2}\times\left[B_2(q)E_{s\pm}(q)-\frac{B_1(q)}{E_{s\pm}(q)}\right] , \qquad M_a(q)=\frac{\alpha_0\Delta^3}{\sqrt{\Delta_s^4-\alpha_0\Delta^4L(q,0)}} \ , \tag{A7}$$

$$A_1=\Delta_a^4\{1-\alpha_0L(q,0)\} \ , \qquad A_2=\Delta_a^2-\frac{\Delta}{2}\alpha_0\Delta_aL(q,0)+\frac{\{h\Delta\alpha_0L(q,0)\}^2}{8\Delta_s^2} \ , \qquad B_1(q)=\alpha_0\Delta_a^3 \ , \qquad B_2(q)=\alpha_0\left[\Delta_a+\frac{\alpha_0\Delta h^2}{2\Delta_s^2}L(q,0)\right] . \tag{A8}$$

In this case, three excitation modes appear in contrast to (A3b), because $\chi_f^{(0)zz}$ is nonzero in a field perpendicular to the z axis.

[1] J. Jensen and A. R. Mackintosh, *Rare Earth Magnetism* (Clarendon, Oxford, 1991).
[2] K. Andres and O. V. Lounasmaa, *Progress in Low Temperature Physics*, edited by D. F. Brewer (North-Holland, Amsterdam, 1982), Vol. VIII.
[3] R. M. White and P. Fulde, Phys. Rev. B **47**, 1540 (1981).
[4] P. Fulde and J. Jensen, Phys. Rev. B **27**, 4085 (1983).
[5] E. M. Forgan, Physica B **107**, 65 (1981).
[6] M. Wulff, G. G. Lonzarich, D. Fort, and H. L. Skriver, Europhys. Lett. **7**, 629 (1988).
[7] H. Ishii, Jpn. J. Appl. Phys. Suppl. **26**, 429 (1988).
[8] H. Ishii, Prog. Theor. Phys. Suppl. **101**, 197 (1990).
[9] H. Ishii and K. Akai, J. Magn. Magn. Mater. **104-107**, 1457 (1992).
[10] S. Doniach and S. Engelsberg, Phys. Rev. Lett. **17**, 750 (1966).
[11] W. F. Brinkman and S. Engelsberg, Phys. Rev. **169**, 169 (1968).
[12] W. Brenig, H. Mikeska, and E. Riedel, Z. Phys. **206**, 439 (1967).
[13] J. Jensen and A. K. Mackintosh, *Rare Earth Magnetism*, Ref. 1, pp. 46–50.
[14] H. Miwa, Prog. Theor. Phys. **34**, 1040 (1965).
[15] J. G. Houmann, B. D. Rainford, J. Jensen, and A. R. Mackintosh, Phys. Rev. B **20**, 1105 (1979).
[16] S. Takayanagi, N. Wada, T. Watanabe, Y. Onuki, and T. Komatubara, J. Phys. Soc. Jpn. **57**, 3552 (1988).
[17] T. Moriya, J. Phys. Soc. Jpn. **18**, 516 (1963).